Global failure probability function estimation based on an adaptive strategy and combination algorithm

Xiukai Yuan[a,*], Yugeng Qian[a], Jingqiang Chen[a], Matthias G.R. Faes[b,**], Marcos A. Valdebenito[b], Michael Beer[d,e,f]

[a] *School of Aerospace Engineering, Xiamen University, Xiamen 361005, P. R. China*
[b] *Chair for Reliability Engineering, TU Dortmund University, Leonhard-Euler-Strasse 5, 44227 Dortmund, Germany.*
[c] *Institute for Risk and Reliability, Leibniz Universität Hannover, Callinstr. 34, Hannover, Germany*
[d] *Institute for Risk and Uncertainty, University of Liverpool, Peach Street, L69 7ZF Liverpool, United Kingdom*
[e] *International Joint Research Center for Resilient Infrastructure & International Joint Research Center for Engineering Reliability and Stochastic Mechanics, Tongji University, Shanghai 200092, China*

Abstract

The failure probability function (FPF) expresses the probability of failure as a function of the distribution parameters associated with the random variables of a reliability problem. Knowledge on this FPF is of much relevance for reliability sensitivity analysis and reliability-based design optimisation. However, its calculation is usually a challenging task. Therefore, this paper presents an efficient approach for estimating the FPF based on on an adaptive strategy and a combination algorithm. The proposed approach involves three basic elements: 1) a Weighted Importance Sampling approach, which allows determining local FPF estimates; 2) an adaptive strategy for determining at which realisations of the distribution parameters it is necessary to perform local FPF estimation; and 3) an optimal combination algorithm, which allows to aggregate local FPF estimations together to form a global estimate of the FPF. Test and practical examples are presented to demonstrate the efficiency and feasibility of the proposed approach.

Keywords: Failure probability function, Importance Sampling, Combination algorithm, Adaptive strategy

1. Introduction

Recent advances in computational mechanics allow to explicitly model the unavoidable effects of uncertainty on the performance of engineering systems [1]. Typically, one is interested in assessing the reliability of the system through metrics such as the failure probability, including either its sensitivity [2] or even optimising the system's design considering its level of reliability [3]. In all of the aforementioned cases, it is of importance to determine the relation between the probability of failure and the distribution parameters associated with the random variables of a reliability problem. Such relation has been termed in the literature as the Failure Probability Function (FPF). The main objective of this work is to propose an efficient numerical procedure for approximating this FPF.

The current approaches for FPF estimation can be roughly grouped into three classes. The first class comprises surrogate modelling approaches. In essence, a surrogate models involves selecting some predefined interpolation points in the space of the distribution parameters by means of design of experiments. Then, reliability analyses are carried on these interpolation points, allowing to train the surrogate model. For example, Gasser [4] adopts a predefined quadratic function to approximate the logarithm of FPF. Jensen [5] adopted a linear function to approximate the logarithm of FPF. Note that other types of surrogate model methods such as Kriging [6, 7], Support vector machine [8, 9], etc., which are widely applied in reliability analysis to approximate the limit state function [10, 11], can be also used to approximate the FPF. The second class of approaches provides a *local* approximation of the FPF with respect to distribution parameters by performing a standard reliability analysis. In this context, *local* implies that the approximation of the FPF is valid over a small neighbourhood around an expansion point. For example, Zou and Mahadevan [12] expressed the FPF as a linear function of the distribution parameters by applying a first-order Taylor series about an expansion point based on reliability sensitivity information. Yuan [13] proposed a weighted approach to obtain the FPF. In the latter approach, the estimate of FPF is expressed as a function of a set of samples of the distribution parameters which are generated in a single reliability analysis. Further, an advanced Line sampling approach is proposed to solve the FPF in [14], which is similar to the weighted approach, as it only needs one simulation run of Line Sampling. The third class of strategies for estimating the FPF involves the formulation of the reliability problem in an augmented space. The seminal work of Au [15] proposes to calculate the FPF by using the Bayes' rule and a single augmented reliability analysis. In this context, *augmented* implies that distribution parameters are modelled as random variables. Naturally, this is just a convenient artefact that allows applying the Bayes' rule. Ching and Hsieh [16, 17] follow the augmented reliability idea and adopted the maximum entropy principle to estimate the posterior distribution associated with distribution parameters. Taflanidis and Beck [18] perform minimisation of the FPF in the augmented space by means of stochastic search. Feng et al. [19] investigates the application of augmented space in conjunction with a binning algorithm. Ling et al. [20] also apply the augmented space idea, and combine adaptive Kriging with Monte Carlo simulation to estimate the FPF. Yuan and coworkers [21] further developed the aforementioned concept to estimate the FPF with respect to distribution parameters by sample average which can relieve the distribution fitting step. Zhang et al. [22] proposed an ensemble model method based on Bayes' rule and augmented theory for estimating the FPF by using a weighted form to combine numerous surrogate models.

As noted from the above discussion, approximating the FPF has been a topic of active research. Despite all progresses made, there are still open issues which require further research. For example, the first class of methods produces an approximation of the FPF estimator without additional information regarding its precision. The second class of methods actually provides a local approximation of FPF, which may lack accuracy for some problems, especially when the design space associated with the distribution parameters is large. Finally, the third class of methods may not be suitable for problems which involve a considerable number of distribution parameters. Therefore, in this contribution, a *global* FPF estimation based on Adaptive strategy and Combination algorithm (AC) is proposed. AC consists of the following three key elements.

1. The weighted approach developed in [13] is adopted as fundamental simulation tool to obtain a local approximation of the FPF about specified values of distribution parameters.
2. An optimal combination algorithm is proposed to aggregate local FPF estimations together to form the global FPF estimator.
3. An adaptive strategy is proposed to actively determine the values of distribution parameters at which the local FPF estimation is carried out. This adaptive strategy is actually an active search which seeks to minimise an error measure.

Note that it is worth pointing out the differences between the proposed approach with various Importance Sampling (IS) methods. It has been observed in [20, 23] that most IS methods address the computation of failure probability for specific values of the distribution parameters of a reliability problem. Weighted Importance Sampling (WIS) [13] extends the traditional IS approach by introducing an instrumental IS density function that admits a range of values for the distribution parameters of a reliability problem. In that way, it is possible to determine a closed-form estimator for the FPF. However, WIS is typically a local approximation method. Therefore, the adaptive strategy and an optimal combination algorithm proposed in this work allow to extend its capability from local estimation to global estimation. In this sense, the proposed approach can be seen as an extended version of the weighted approach reported in [13].

This contribution is organised as follows. In Section 2, the formal definition of FPF estimation is briefly presented. Then, the mathematical formulation of the proposed framework is developed in Section 3. In Section 4, various examples are presented to show the performance of the proposed approach. Finally, Section 5 lists the conclusions of the paper.

2. Problem definition

The objective of this contribution is calculating failure probability as a function of distribution parameters associated with the random variables of a reliability problem. This is termed as failure probability function (FPF) and is denoted as $P_F(\boldsymbol{\theta})$, where P_F denotes failure probability; $\boldsymbol{\theta} = [\theta_1, \cdots, \theta_{n_\theta}] \in \mathcal{S}$ is the vector of distribution parameters and $\mathcal{S}$ the hyper-rectangular design space to which the distribution parameters belong to. Note that $\mathcal{S}$ is bounded either by the physics of the problem under consideration or by a priori considerations. In addition, note that the vector of distribution parameters $\boldsymbol{\theta}$ can be also interpreted as a design vector [3].

The failure probability function $P_F(\boldsymbol{\theta})$ is defined as:

$$P_F(\boldsymbol{\theta}) = \int I_F(\boldsymbol{x}) f(\boldsymbol{x} \mid \boldsymbol{\theta}) \mathrm{d}\boldsymbol{x}, \tag{1}$$

where $\boldsymbol{x}$ is a vector-valued realisation of the random variable vector $\boldsymbol{X}$ that characterises the uncertain inputs of a reliability problem; $f(\boldsymbol{x} \mid \boldsymbol{\theta})$ is the PDF of $\boldsymbol{X}$ conditioned on the distribution parameters $\boldsymbol{\theta}$; and $I_F(\boldsymbol{x})$ is the indicator function, which assumes the value $I_F(\boldsymbol{x}) = 1$ if $\boldsymbol{x} \in F$ and $I_F(\boldsymbol{x}) = 0$ otherwise. Note that F represents the failure domain associated with the realisations of the random variable vector. It is defined as $F = \{\boldsymbol{x} : g(\boldsymbol{x}) < 0\}$, where $g(\boldsymbol{x})$ is the performance function, which assumes a value equal or smaller than zero in case that the realisation $\boldsymbol{x}$ of the uncertain input parameters causes an unacceptable system's behaviour. Inspection of the above equation indeed reveals that, in order to fully map $P_F(\boldsymbol{\theta})$, a full reliability analysis is required for each $\boldsymbol{\theta} \in \mathcal{S}$.

3. Proposed approach for global FPF estimation

3.1. Overview of the proposed approach

This section presents the proposed approach to estimate the FPF efficiently with high global accuracy, which is based on an adaptive strategy and a combination algorithm. The global FPF estimator $\hat{P}_{F,C}^{(k)}(\boldsymbol{\theta})$ is obtained by combining a number of k local estimators, and is explicitly given by:

$$\hat{P}_{F,C}^{(k)}(\boldsymbol{\theta}) = \sum_{i=1}^{k} w_i(\boldsymbol{\theta})\hat{P}_F^{(i)}(\boldsymbol{\theta}), \tag{2}$$

where $\hat{P}_F^{(i)}(\boldsymbol{\theta})$ is the $i-th$ local estimator, whose calculation is explained in detail in Section 3.2; k is the total number of different local estimators; and $w_i(\boldsymbol{\theta})$ is a weight function. Note that $\sum_{i=1}^{k} w_i(\boldsymbol{\theta}) = 1$ is imposed for each value of $\boldsymbol{\theta}$. Thus, as long as $\hat{P}_F^{(i)}(\boldsymbol{\theta})$ is unbiased, then the obtained $\hat{P}_{F,C}(\boldsymbol{\theta})$ is also unbiased. The exact values of each $w_i(\boldsymbol{\theta})$ are obtained via a combination algorithm, as explained in detail in Section 3.3. Furthermore, the identification of the realisations of $\boldsymbol{\theta}$ at which a local FPF estimator is required is carried out by means of active learning, as described in detail in Section 3.4.

Before continuing, it is useful to derive some properties of the global FPF estimator shown in Eq. 2. In case that the FPF components, $\hat{P}_F^{(i)}(\boldsymbol{\theta})$, are mutually independent, the variance of $\hat{P}_{F,C}^{(k)}(\boldsymbol{\theta})$ can be easily obtained by

$$Var\left[\hat{P}_{F,C}^{(k)}(\boldsymbol{\theta})\right] = \sum_{i=1}^{k} w_i^2(\boldsymbol{\theta}) Var\left[\hat{P}_F^{(i)}(\boldsymbol{\theta})\right] \tag{3}$$

Further, if all the FPF components, $\hat{P}_F^{(i)}(\boldsymbol{\theta})$, are unbiased estimators, i.e., $E[\hat{P}_F^{(i)}(\boldsymbol{\theta})] = P_F(\boldsymbol{\theta})$, then the coefficient of variation (C.o.V.) of $\hat{P}_{F,C}^{(k)}(\boldsymbol{\theta})$ is given by

$$Cov[\hat{P}_{F,C}^{(k)}(\boldsymbol{\theta})] = \frac{\sqrt{\sum_{i=1}^{k} w_i(\boldsymbol{\theta})^2 Var[\hat{P}_F^{(i)}(\boldsymbol{\theta})]}}{P_F(\boldsymbol{\theta})} = \sqrt{\sum_{i=1}^{k} w_i^2(\boldsymbol{\theta}) Cov^2[\hat{P}_F^{(i)}(\boldsymbol{\theta})]} \tag{4}$$

3.2. Local estimate of FPF by the weighted approach

A local estimate of the FPF is produced by means of the Weighted Importance Sampling (WIS) approach presented in [13]. The first step of WIS consists of introducing an instrumental probability density function $H(\boldsymbol{x})$. Then, the FPF in Eq. (1) is rewritten as:

$$P_F(\boldsymbol{\theta}) = \int \frac{I_F(\boldsymbol{x}) f(\boldsymbol{x} \mid \boldsymbol{\theta})}{H(\boldsymbol{x})} H(\boldsymbol{x}) \mathrm{d}\boldsymbol{x} \tag{5}$$

which is further expressed as:

$$P_F(\boldsymbol{\theta}) = E_H\left[\frac{I_F(\boldsymbol{x}) f(\boldsymbol{x} \mid \boldsymbol{\theta})}{H(\boldsymbol{x})}\right] = E_H\left[I_F(\boldsymbol{x}) r(\boldsymbol{x}, \boldsymbol{\theta})\right] \tag{6}$$

where $r(\boldsymbol{x},\boldsymbol{\theta}) = f(\boldsymbol{x} \mid \boldsymbol{\theta})/H(\boldsymbol{x})$ is the ratio of two distributions. Assume that N samples are generated according to $H(\boldsymbol{x})$, that is, $\{\boldsymbol{x}^{(j)}, j = 1, \ldots, N\}$. Then, the FPF can be estimated as:

$$\hat{P}_F(\boldsymbol{\theta}) = \frac{1}{N} \sum_{j=1}^{N} \frac{I_F\left(\boldsymbol{x}^{(j)}\right) f\left(\boldsymbol{x}^{(j)} \mid \boldsymbol{\theta}\right)}{H\left(\boldsymbol{x}^{(j)}\right)} \tag{7}$$

The above equation provides a generic expression for the local approximation of the FPF produced by means of Weighted Importance Sampling. For the $i-th$ $(i = 1, 2, \ldots, k)$ local estimator of the FPF, an Importance Sampling Density (ISD) function $H(\boldsymbol{x})$ is established around the support point $\boldsymbol{\theta}_H^{(i)}$. Specifically, the so-called ISD based on the design point [24] is considered here, which is given as:

$$H(\boldsymbol{x}) = H\left(\boldsymbol{x} \mid \boldsymbol{x}^{*(i)}\right) \tag{8}$$

where $\boldsymbol{x}^{*(i)}$ is the design point solved according to the current support parameter point $\boldsymbol{\theta} = \boldsymbol{\theta}_H^{(i)}$, that is, when $\boldsymbol{x}$ is distributed as $f(\boldsymbol{x} \mid \boldsymbol{\theta}_H^{(i)})$.

Suppose that a number of $N^{(i)}$ samples are generated according to $H\left(\boldsymbol{x} \mid \boldsymbol{x}^{*(i)}\right)$, i.e., $\{\boldsymbol{x}^{(j)} \sim H\left(\boldsymbol{x} \mid \boldsymbol{x}^{*(i)}\right), j = 1, \ldots, N^{(i)}\}$. According to Eq. (6), $P_F(\boldsymbol{\theta})$ can be estimated based on these samples by

$$\hat{P}_F^{(i)}(\boldsymbol{\theta}) = \frac{1}{N} \sum_{j=1}^{N} \frac{I_F\left(\boldsymbol{x}^{(j)}\right) f\left(\boldsymbol{x}^{(j)} \mid \boldsymbol{\theta}\right)}{H\left(\boldsymbol{x}^{(j)} \mid \boldsymbol{x}^{*(i)}\right)} \tag{9}$$

Obviously, the estimator in Eq. (9) is unbiased for each value of $\boldsymbol{\theta}$. The corresponding variance and coefficient of variation are given by

$$Var[P_F^{(i)}(\boldsymbol{\theta})] \approx \frac{1}{N-1} \left\{ \frac{1}{N} \sum_{j=1}^{N} \left[\frac{I_F\left(\boldsymbol{x}^{(j)}\right) f\left(\boldsymbol{x}^{(j)} \mid \boldsymbol{\theta}\right)}{H\left(\boldsymbol{x}^{(j)} \mid \boldsymbol{x}^{*(i)}\right)} \right]^2 - [\hat{P}_F^{(i)}(\boldsymbol{\theta})]^2 \right\} \tag{10}$$

$$Cov[P_F^{(i)}(\boldsymbol{\theta})] = \frac{\sqrt{Var[\hat{P}_F^{(i)}(\boldsymbol{\theta})]}}{P_F(\boldsymbol{\theta})} \approx \frac{\sqrt{Var[\hat{P}_F^{(i)}(\boldsymbol{\theta})]}}{\hat{P}_F^{(i)}(\boldsymbol{\theta})} \tag{11}$$

The local estimate of FPF in Eq. (9) provides sufficient accuracy when $\boldsymbol{\theta}$ is near the current support parameter point $\boldsymbol{\theta}_H^{(i)}$. However, it may show a large coefficient of variation for values of $\boldsymbol{\theta}$ far from $\boldsymbol{\theta}_H^{(i)}$. The latter is undesirable, as it may imply considerable error in the prediction of the FPF and can be particularly problematic for large design spaces $\mathcal{S}$. Such issue can be circumvented by means of a combination algorithm, which is explained in the following.

3.3. Combination algorithm

An optimal Combination algorithm is proposed to determine the weights function $w_i(\boldsymbol{\theta})$ in Eq. (2). Note that the performance of Combination algorithm depends highly on the calculated weights, and hence, the approach used to calculate these weights is highly influential. There are three approaches for combination algorithm proposed in this paper: (1) equal weights; (2) determination of an optimal $w_i(\boldsymbol{\theta})$ that minimises the variance of $\hat{P}_{F,C}^{(i)}(\boldsymbol{\theta})$; and (3) determination of an optimal $w_i(\boldsymbol{\theta})$ that minimises the C.o.V. of $\hat{P}_{F,C}^{(i)}(\boldsymbol{\theta})$. These approaches are discussed and evaluated in the following.

3.3.1. Combination based on average weights

The most straightforward way to combine the local approximations of FPF is to add them considering equal weights, that is

$$w_i(\boldsymbol{\theta}) = \frac{1}{k} \quad (i = 1, \cdots, k) \tag{12}$$

Generally, the combination based on average weights is quite easy to apply. However, it may provide poor estimates in other cases, as discussed later on.

3.3.2. Optimal combination based on minimising the variance

A set of optimal weights can be selected such that the variance of the FPF estimator $\hat{P}_{F,C}^{(k)}(\boldsymbol{\theta})$, as given in Eq. (2), is minimised. As explained in detail in Appendix A, the optimal weights that fulfill such criterion are:

$$w_i(\boldsymbol{\theta}) = \frac{Var^{-1}\left[\hat{P}_F^{(i)}(\boldsymbol{\theta})\right]}{\sum_{j=1}^{k} Var^{-1}\left[\hat{P}_F^{(j)}(\boldsymbol{\theta})\right]} \quad (i = 1, \cdots, k) \tag{13}$$

This equation shows that the optimal weight associated with $\hat{P}_F^{(i)}(\boldsymbol{\theta})$ decreases with increase of the variance of $\hat{P}_F^{(i)}(\boldsymbol{\theta})$. Furthermore, substitution of Eq. (13) into Eq. (3), yields the variance of the estimate for the FPF, which is equal to

$$Var[\hat{P}_{F,C}^{(k)}(\boldsymbol{\theta})] = \frac{1}{\sum_{i=1}^{k} Var^{-1}[\hat{P}_F^{(i)}(\boldsymbol{\theta})]} \tag{14}$$

3.3.3. Optimal combination based on minimising the C.o.V.

The third approach consists of determining the weights such that $\hat{P}_{F,C}^{(k)}(\boldsymbol{\theta})$ possesses the smallest C.o.V. The optimal weights are then given by:

$$w_i(\boldsymbol{\theta}) = \frac{Cov^{-2}\left[\hat{P}_F^{(i)}(\boldsymbol{\theta})\right]}{\sum_{j=1}^{k} Cov^{-2}\left[\hat{P}_F^{(j)}(\boldsymbol{\theta})\right]} \quad (i = 1, \cdots, k) \tag{15}$$

The detailed derivation of Eq. (15) is presented in Appendix A. Eq. (15) shows that the optimal weight of $\hat{P}_F^{(i)}(\boldsymbol{\theta})$ decreases with increase of the C.o.V. of $\hat{P}_F^{(i)}(\boldsymbol{\theta})$.

Furthermore, substitution of Eq. (15) into Eq. (4) yields the final C.o.V. of the estimate of FPF, which is equal to:

$$Cov[\hat{P}_{F,C}^{(k)}(\boldsymbol{\theta})] = \frac{1}{\sqrt{\sum_{i=1}^{k} Cov^{-2}[\hat{P}_F^{(i)}(\boldsymbol{\theta})]}} \tag{16}$$

Since $Cov[\hat{P}_F^{(i)}(\boldsymbol{\theta})] \neq 0$, thus $Cov[\hat{P}_F^{(i)}(\boldsymbol{\theta})]^2 > 0$, then it is easy to further deduce that:

$$Cov[\hat{P}_{F,C}^{(k)}(\boldsymbol{\theta})] \leq Cov[\hat{P}_F^{(i)}(\boldsymbol{\theta})], (i = 1, \cdots, k) \tag{17}$$

which means that the combined estimate will own the smallest C.o.V. in theory compared with the local estimates of the FPF.

It should be noted that the optimal weights in Eqs. (13) and (15) depend on variance and co-variance, which are not available in closed form. In this case, the corresponding sample estimators could be used instead, but would introduce bias in the estimation, as discussed in [25]. However, the estimates presented in the paper are *biased but consistent*, which means that they will converge asymptotically to the correct value as the number of samples involved increases. This point is demonstrated through a lemma given in Appendix B and a test example in Subsection 4.1, which confirms that this effect is negligible for the purposes of this work.

3.3.4. Comparison of criteria for combination

A two-dimensional academic example is given to illustrate the three different combination criteria described previously. Suppose that the limit state function is given as $g(\boldsymbol{x}) = 4 - x_1 - x_2$, where $x_1 \sim N(\theta, 1)$, $x_2 \sim N(0, 1)$ are the basic random variables, and $\theta \in [-2, 2]$ is the distribution parameter for which the FPF is sought. Weighted Importance Sampling is applied twice, each time considering one of the following two design points: $\boldsymbol{x}_L^* = [1, 3]$ and $\boldsymbol{x}_U^* = [3, 1]$. It can be shown that these two are the design points when the distribution parameter is set as $\theta = -2$ and $\theta = 2$, respectively. Each implementation of Weighted Importance Sampling (WIS) is carried out using $N = 100$ samples. The results by different settings and methods are plotted in Fig. 1. In this figure, 'WIS($\boldsymbol{x}_L^*$)' and 'WIS($\boldsymbol{x}_U^*$)' denote the weighted approach with sampling centres on $\boldsymbol{x}_L^*$ and $\boldsymbol{x}_U^*$, respectively; 'Average weights', 'Variance weights' and 'C.o.V. weights' denotes the combination based on average weights, minimising the variance of $\hat{P}_F^{(k)}(\theta)$ and the C.o.V. of $\hat{P}_F^{(k)}(\theta)$, respectively. Note that these combination estimators are constructed based on the two independent simulations of WIS, that is, $k = 2$.

It can be seen from Fig. 1 that the local FPF estimates obtained by means of WIS (that is, WIS($\boldsymbol{x}_U^*$) and WIS ($\boldsymbol{x}_L^*$)) can possess a large coefficient of variation. The approaches that combine the two local estimates of the FPF by means of weights exhibit a smaller coefficient of variation. Among these, the approach that uses weights that minimise the C.o.V exhibits the best accuracy. Based on this observation, in this work, only the combination algorithm based on minimising the C.o.V. is adopted and further investigated.

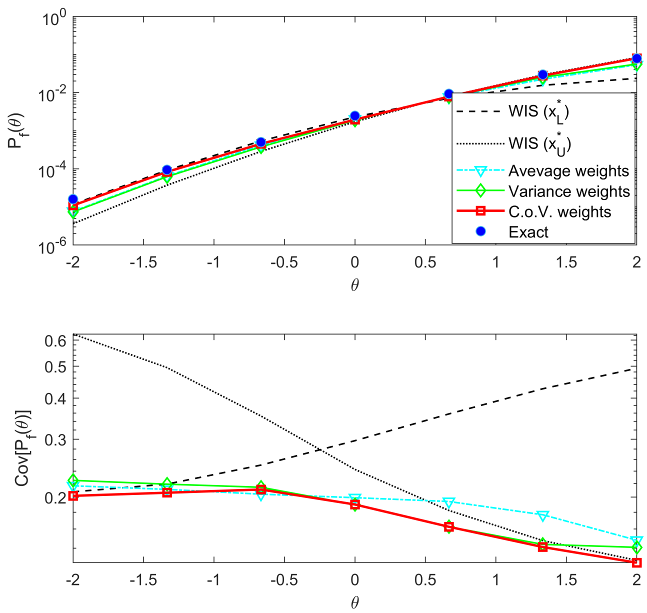

Figure 1: Comparison of the FPF estimators and C.o.V.'s by different ways.

3.4. *Adaptive strategy*

The above discussion has addressed the construction of a local estimate of the FPF (see Section 3.2) as well as the aggregation of different local FPF into a combined estimator (see Section 3.3). Nonetheless, the issue on how to select the support point $\boldsymbol{\theta}_H^{(i)}(i = 2, 3, \ldots, k)$ for constructing a local approximation $\hat{P}_F^{(i)}(\boldsymbol{\theta})$ remains open. In principle, these support points can be selected a priori, e.g., through a predefined experimental design heuristics, like centre design, or following random approaches, such as MCS, Latin Hypercube Sampling (LHS) or other low-discrepancy sequences. However, such a priori experimental design may not be the most efficient approach. Hence, a novel way to determine the location of the support points associated with the construction of the local FPF estimators based on active learning is developed here. Since the C.o.V. is a good estimator of the precision of an estimator, the C.o.V. of the aggregated global FPF estimator is used as a learning function to select the next support point for constructing a new local FPF estimate to augment (or improve) the quality of the current global estimate. Specifically, the point $\boldsymbol{\theta} \in \mathcal{S}$ that possesses the largest value of C.o.V. should be chosen as the next support point.

Suppose that the $i-th$ estimator of the FPF $\hat{P}_{F,C}^{(i)}(\boldsymbol{\theta})$ is calculated according to Eq. (2), and the C.o.V. of the estimator is obtained according to Eq. (4), then the next support parameter point $\boldsymbol{\theta}_H^{(i+1)}$ is determined by solving the following optimisation problem:

$$\begin{aligned} \text{Find} \quad & \boldsymbol{\theta}_H^{(i+1)} = \boldsymbol{\theta}_{\max} \\ \text{Max} \quad & Cov[\hat{P}_{F,C}^{(i)}(\boldsymbol{\theta})] \\ \text{s.t.} \quad & \underline{\theta}_j \leq \theta_j \leq \overline{\theta}_j \quad (j = 1, 2, \ldots, n_\theta)\,. \end{aligned} \tag{18}$$

where $\underline{\theta}_j$ and $\overline{\theta}_j$ denote the lower and upper bounds for θ_j. Note that this optimisation problem does not involve any evaluation of limit state function. Thus, it can be readily solved by adopting any appropriate optimisation algorithm. In this contribution, the optimisation problem in Eq. (18) is solved by means of MCS, as its implementation is quite straightforward. When the dimension of $\boldsymbol{\theta}$ is large (i.e., larger than 10), other algorithms, e.g., Particle Swarm Optimisation, can be used to solve Eq. (18).

Note that active strategy in Eq. (18) can be repeated, until convergence is reached. The stopping criterion can be selected as $\max\left(Cov[\hat{P}_F(\boldsymbol{\theta})]\right) \leq c_{tol}$, where c_{tol} is a given tolerance value.

3.5. Summary of the proposed approach

The proposed approach to estimate the global FPF in an active way can be summarised in the following steps, which are also depicted in a flow diagram in Fig. 2.

1. Initialise design. Set $i = 1$. Choose an initial value of $\boldsymbol{\theta}_H^{(1)}$. A possible choice is $\boldsymbol{\theta}_H^{(1)} = (\overline{\boldsymbol{\theta}} - \underline{\boldsymbol{\theta}})/2$, where $\overline{\boldsymbol{\theta}}$ and $\underline{\boldsymbol{\theta}}$ denote the maximum and minimum values that $\boldsymbol{\theta}$ may assume.
2. Carry out Weighted Importance Samplig (WIS). Based on the Importance Sampling density function, $H(\boldsymbol{x})$ given in Eq. (8) and the support point $\boldsymbol{\theta}_H^{(i)}$, produce samples $\left\{\boldsymbol{x}^{(j)} : j = 1, \ldots, N\right\}$. The local FPF estimator is established by means of Eq. (9).
3. Produce the global FPF estimator with the optimal combination algorithm. Calculate the weights according to Eq. (15), and then produce the global FPF estimate following Eq. (2).
4. Determine the next support parameter point by active learning. Solve the optimisation problem in Eq. (18) to obtain next support parameter point $\boldsymbol{\theta}_H^{(i+1)}$.

5. In case that the maximum coefficient of variation of the global FPF estimate is above the tolerance c_{tol}, return to step 2 with $i = i + 1$. Otherwise, stop the iteration.

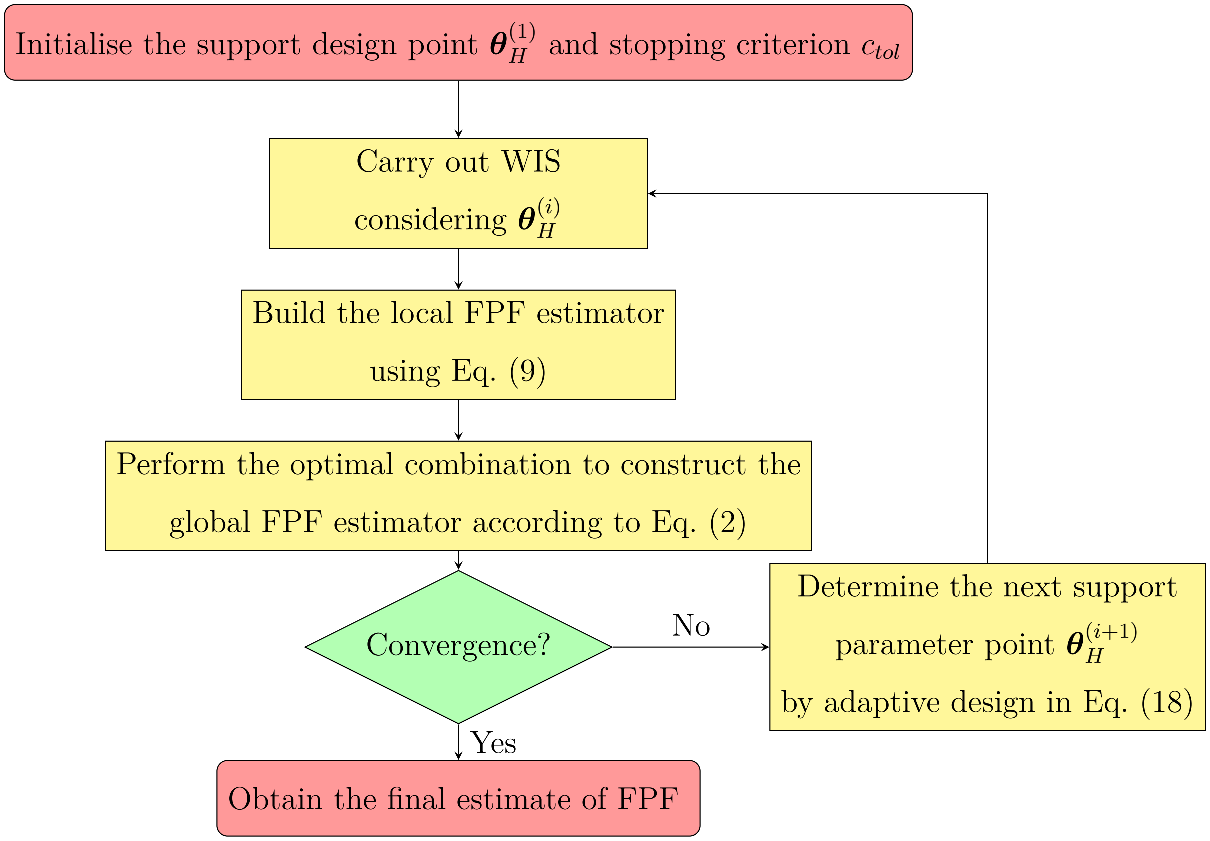

Figure 2: Flowchart of the proposed approach.

4. Examples

In this section, three examples are presented to illustrate the performance of the proposed approach. These examples are solved by means of three different approaches:

(a) The proposed approach (which is denoted as AC) with weights selected such that the C.o.V. of the global FPF estimate is minimised, as described in Section 3.3.3.

(b) The WIS approach, which corresponds to a local FPF estimation [13]. Note that this approach is described in Section 3.2.

(c) An augmented space integral (ASI) approach implemented with Importance Sampling, as proposed in [14]. It produces a global FPF estimation through reliability analysis in an augmented reliability space.

Note that these selected approaches are comparable between them, as they are simulation-based methods where the corresponding C.o.V. of FPF is available. Note that methods based on response surface (or surrogate model) [5] or the augmented space method with density fitting [16] are not included in the comparison. Such decision is made as the latter methods require additional assumptions and they do not produce information on the C.o.V. of the probability estimates. Direct MCS and IS are also applied to obtain the point-wise values of failure probability which are regarded as the 'exact values'. The optimisation problem in Eq. (18) is solved by random search using MCS. The stopping criterion $c_{tol} = 0.2$ is set for all the examples.

4.1. Example 1: A test example

The first example considers a simple limit state function, which is given by

$$g(\boldsymbol{x}) = 1 + \exp(-0.5x_1) - x_2 \tag{19}$$

where x_1 and x_2 are normal distributed random variables, i.e., $x_1 \sim N(\theta_1, 1)$ and $x_2 \sim N(\theta_2, 1)$, where the mean values of x_1 and x_2 are taken as the design parameters, and the design domains are $\theta_1 \in [-2.5, 2.5]$ and $\theta_2 \in [-2.5, 2.5]$.

4.1.1. Results of the proposed approach

The proposed approach is applied to estimate the global FPF of this problem. First $\boldsymbol{\theta}_H^{(1)} = [-2.5, -2.5]$ is set, which is located in the lower bound of the design region. Then, the corresponding design point $\boldsymbol{x}^{*(1)} = [0.4851, 1.8646]$ is determined, and WIS based on this design point is performed with $N = 100$ samples. Note that the design point is solved by using Advance First Order and Second Moment (AFOSM) [26] method and 30 evaluations of the performance function are required.

Fig. 3 shows the two-dimensional FPF estimates obtained by the proposed method, as well as the two-dimensional C.o.V. of estimator. It can be seen that the final C.o.V. values are all less than 0.2. Further, Fig. 4a and 4b show two one-dimensional projections of the FPF, namely $P_F(\theta_1, \theta_2 = 0)$ and $P_F(\theta_1 = 0, \theta_2)$, with respect to the number of iterations, respectively. Direct MCS is applied with $N = 10^7$ samples for each point-wise value of FPF which is take as the 'exact' value (denoted by 'circle'). It can be seen that the FPF estimate is improved at each step of the iterative process. For example, in Fig. 4a, some error exists in the FPF estimator in the early steps, e.g., over the left and right sides of design region of θ_1. The corresponding C.o.V.s are also large. As the iteration process advances, the results are improved until the stopping criterion is reached.

In order to illustrate the effectiveness of the adaptive design, the C.o.V. of the estimator in each iteration, as well as the support parameter points $\boldsymbol{\theta}_H^{(i)} (i = 1, ..., 4)$ determined by the adaptive strategy, are shown in Fig. 5. The support points which are also the points with the biggest C.o.V. values in each iteration are shown in the figure (denoted by red dots). It can be noted that the C.o.V. of the estimator monotonically decreases as the iteration process continues.

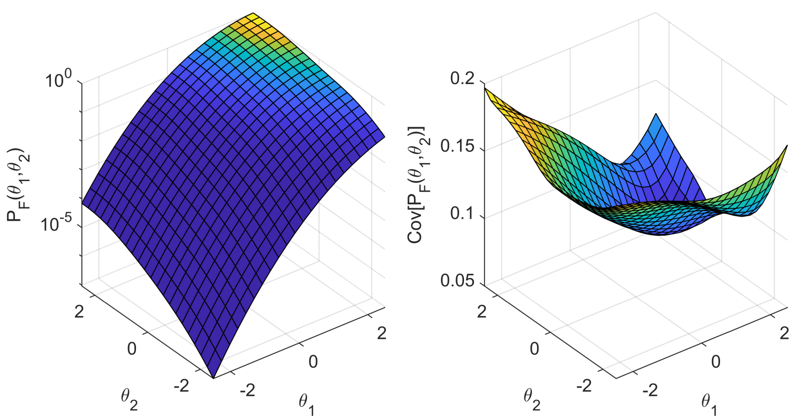

Figure 3: The FPF results by the proposed approach (Example 1).

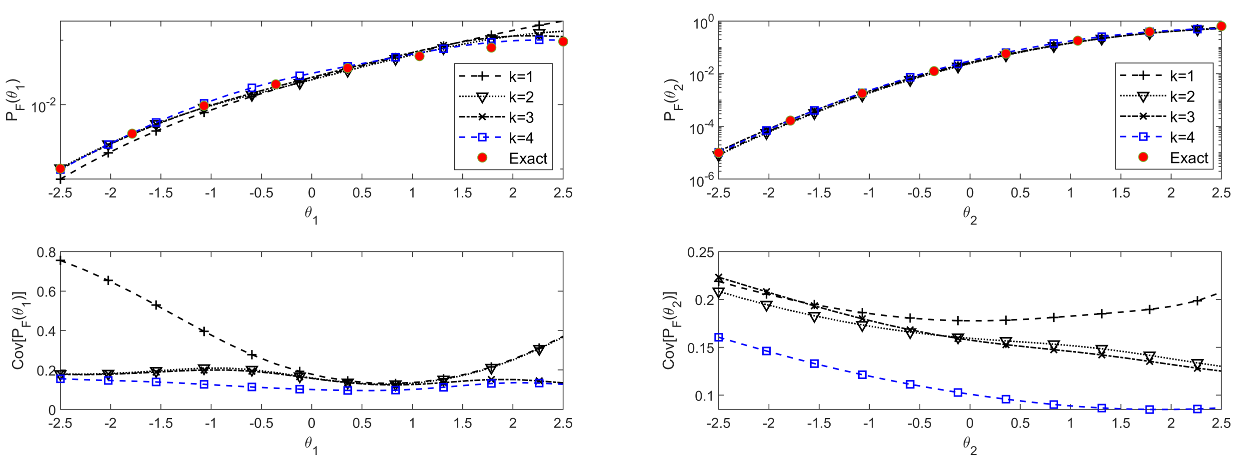

(a) $P_F(\theta_1, \theta_2 = 0)$

(b) $P_F(\theta_1 = 0, \theta_2)$

Figure 4: The one-dimensional FPF results by the proposed method (Example 1).

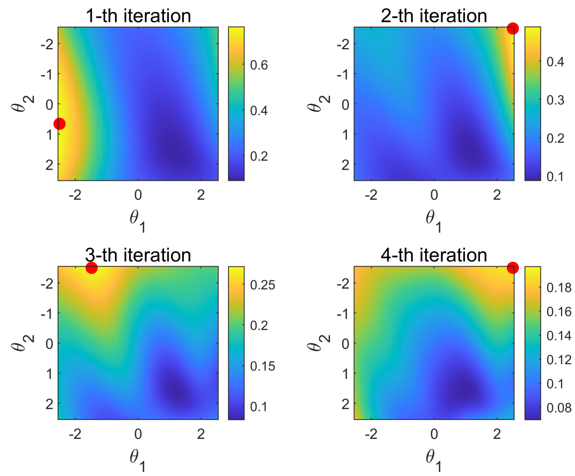

Figure 5: The C.o.V.s of the FPF results in each iteration by the proposed approach (Example 1). The red points denote the locations of $\boldsymbol{\theta}_H^{(k+1)}(k = 1, ..., 4)$.

4.1.2. Comparison with other methods

The proposed method is compared with WIS and ASI in this subsection. First, all these methods are implemented with the same number of simulated samples, i.e., $N_T = N \times k = 100 \times 4$ for the proposed approach, and $N = 400$ for the WIS and ASI-IS. The design point $\boldsymbol{x}^{*(1)}$ in the proposed approach is also used for WIS and ASI. Note that the computation cost of solving the design point is not included here since it is negligible compared to the limit state function evaluations in these approaches.

Fig. 6a and 6b shows the one dimensional FPF results (as well as their C.o.V. estimators). It can be seen in Fig. 6a that the FPF result of AC is consistent with the 'Exact' results by direct MCS, while those of both ASI and WIS posses considerable error when $\theta_1 \in [-2.5, -0.5]$. In both figures, ASI has the largest C.o.V. and also the proposed approach obtains the smoothest C.o.V. which owns the smallest maximum value of C.o.V. over the design region.

In addition, all these methods are implemented with the same stop criterion $Cov[\hat{P}_F(\boldsymbol{\theta})] \leq c_{tol} = 0.2$. Table 1 shows the total number of evaluations of the performance function (including the design points identification) by different methods through an average over 10 independent runs. Different initial support parameter points $\boldsymbol{\theta}_H^{(1)}$ are also considered, i.e., (1) initial design 1: $\boldsymbol{\theta}_H^{(1)} = [-2.5, -2.5]$, (2) initial design 2: $\boldsymbol{\theta}_H^{(1)} = [0, 0]$, and (3) initial design 3: $\boldsymbol{\theta}_H^{(1)} = [2.5, 2.5]$. It can be seen that the total number of evaluations of the performance function by WIS varies according to different starting points, i.e., from 5840 to 87100, while those of ASI-IS and are relatively steady. Among them, the proposed method based on an adaptive strategy and combination algorithm (AC) requires the least number of calls to the performance function. This illustrates that, in this case, the proposed approach is more efficient and effective than WIS and ASI-IS.

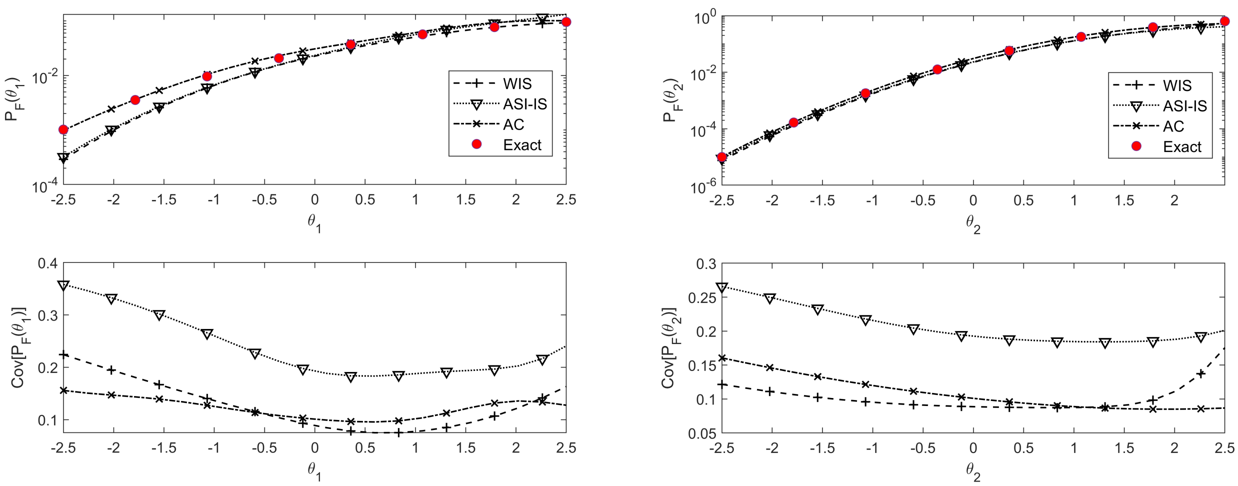

(a) $P_F(\theta_1, \theta_2 = 0)$ (b) $P_F(\theta_1 = 0, \theta_2)$

Figure 6: The one-dimensional FPF results by different methods with the same number of simulated samples N_T (Example 1).

Table 1: Average number of samples for different methods under the same stopping criterion (average results over 10 runs) (Example 1).

Methods	Initial design 1	Initial design 2	Initial design 3
WIS	16640	5840	47070
ASI-IS	3470	3010	2578
AC ($N = 100$)	1270	952	1056

4.1.3. Parametric Analysis

The performance under different settings of the proposed approach is investigated here, i.e., with respect to different numbers of samples (N) and initial support parameter points ($\boldsymbol{\theta}_H^{(1)}$). The proposed approach is carried out considering several repeated runs with a number of samples from 50 to 500, and different initial support parameter point $\boldsymbol{\theta}_H^{(1)}$, i.e., (1) initial design 1: $\boldsymbol{\theta}_H^{(1)} = [-2.5, -2.5]$, (2) initial design 2: $\boldsymbol{\theta}_H^{(1)} = [0, 0]$, and (3) initial design 3: $\boldsymbol{\theta}_H^{(1)} = [2.5, 2.5]$.

Fig. 7 shows the performance of the proposed approach, which gives the total number of iterations with respect to the number of samples used in each iteration and under different initial support parameter points employing the proposed approach. It can be seen that, (1) when the number of samples N increases, the number of iterations k decreases, but the number of simulation samples generated by WIS (denoted as N_T) increases; (2) the total number of evaluations of the performance function N_{all} is first smooth when N is over about 50 to 400 and then increases when $N > 400$. Note that N_{all} includes both the simulation samples and the computational cost of solving the design point in each iteration. In this example, the design point is solved at cost of about 30 to 100 evaluations of the performance function.

It is concluded that the selection of N affects the efficiency of the proposed method. First, it is recommended N is selected according to the stopping criterion, e.g., if $Cov[\hat{P}_F(\boldsymbol{\theta})] < 0.2$ is expected, then N should be large enough to ensure $Cov[\hat{P}_F^{(i)}(\boldsymbol{\theta}_H^{(i)})] < 0.2$. Second, the other relevant factor that needs to be considered is the computational cost of solving the design point involved in the each iteration. It is also recommended that the number of samples N should be larger than the number of calls in solving the design point of the performance function, thus leading to a smaller overall computational cost.

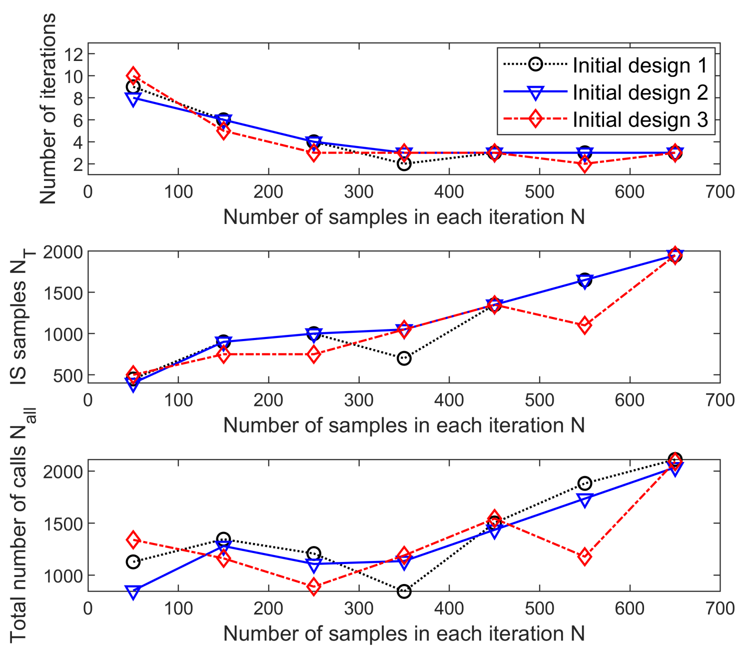

Figure 7: The performance of the the proposed approach with respect to the number of samples used in each iteration and different initial designs (Example 1).

4.1.4. Convergence Analysis

In this subsection, it will be shown that while the results of the proposed AC are biased, this bias is sufficiently small. In this test example, for each value of the distribution parameter vector $\boldsymbol{\theta}$, two independent runs of WIS are carried out, one of which is used for producing the local FPF estimator $\hat{P}_F^{(i)}(\boldsymbol{\theta})$ and the other is used solely for determining the weights $w_{(i)}(\boldsymbol{\theta})$ by means of Eq. (15). By following this approach, the obtained estimator will become immediately unbiased, because the weights are determined using samples which are different (completely independent) from those used for calculating $\hat{P}_F^{(i)}(\boldsymbol{\theta})$. This approach is denoted as 'AC(independent)'.

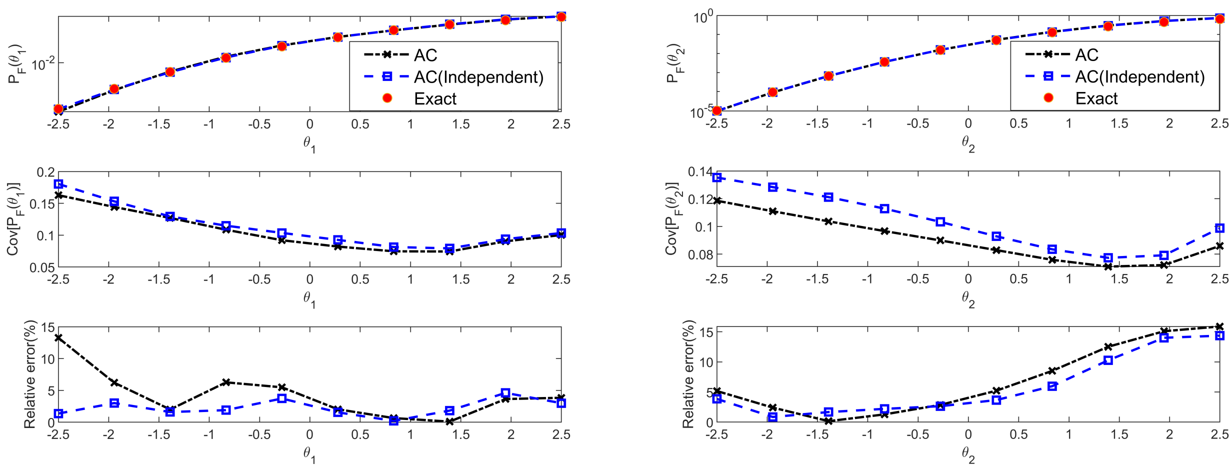

(a) $P_F(\theta_1, \theta_2 = 0)$ (b) $P_F(\theta_1 = 0, \theta_2)$

Figure 8: The one-dimensional FPF results by the proposed AC and AC(independent) when $N = 100$ (Example 1).

Fig. 8 shows the obtained results in one dimension when $N = 100$. The C.o.V. and relative error $\epsilon(\boldsymbol{\theta}) = \frac{|\hat{P}_F(\boldsymbol{\theta}) - P_F^{exact}(\boldsymbol{\theta})|}{P_F^{exact}(\boldsymbol{\theta})}$ where $P_F^{exact}(\boldsymbol{\theta})$ is the exact value calculated by MCS. AC takes a number of $k = 7$ iterations to converge. AC(independent) uses the same information (support parameter points and component FPF estimators) but calculating the weights through a different WIS in each iteration. It can be seen from the figure that the results produced with the unbiased estimator through AC(independent) are almost the same as those of the biased estimator through AC.

4.2. Example 2: Thermal Stress Analysis of Jet Engine Turbine Blade

The second example considers a jet engine turbine blade, as shown in Fig. 9. This blade has interior cooling ducts, through which the flow of cool air maintains the temperature of the blade within the limit for its material. The turbine is a radial array of blades typically made of nickel alloys. These alloys resist the extremely high temperatures of the gases. At such temperatures, the material expands significantly, producing mechanical stress in the joints and significant deformations of several millimetres. To avoid mechanical failure and friction between the tip of the blade and the turbine casing, the blade design must account for the mechanical stresses and deformations. Failure is defined as the maximum von Mises stress of the structure exceeding the given allowable value $\sigma_a = 1.5$GPa, and the corresponding limit state function is:

$$g(\boldsymbol{x}) = \sigma_a - \sigma_{max}(\boldsymbol{x}) \tag{20}$$

where $\sigma_{max}(\boldsymbol{x})$ is the maximum von Mises stress of the blade caused be the combination of thermal and pressure effects; $\boldsymbol{x} = [E, \lambda, \gamma_{CTE}, P_1, P_2, K_{app}, T_1, T_2]$ is the vector of basic random variables; E, λ, γ_{CTE} and K_{app} are the Young's modulus, Poisson's ratio, coefficient of thermal expansion and the thermal conductivity for nickel-based alloy (NIMONIC 90), respectively; P_1 and P_2 are the pressure loads on the pressure and suction sides of the blade which is due to the high-pressure gas surrounding these sides of the blade; T_1 is the temperature of the interior cooling air and T_2 is the temperature on the pressure and suction sides. All these variables are assumed to be independent truncated normal random variables and their distribution parameters are given in Table 2.

There are three distribution parameters which are of interest in this example, namely $\boldsymbol{\theta} = [\mu_E, \mu_{\gamma_{CTE}}, \mu_{T_2}]$, which are the mean values of E, γ_{CTE} and T_2. These parameters are contained within the sets $\theta_1 \in [170, 290]$ (GPa), $\theta_2 \in [10, 18]$ (1/K) and $\theta_3 \in [700, 1300]$(°C), respectively.

The proposed approach is applied to estimate the global FPF of this problem, which is a three-dimensional function. For this purpose, the initial support point is selected as $\boldsymbol{\theta}_H^{(1)} = [170, 10, 700]$ which corresponds to the lower bound of the design region. Then, $N = 300$ is set for constructing each local estimate of the FPF through Weighted Importance Sampling (WIS) considering the support point $\boldsymbol{\theta}_H^{(i)}$ which is selected according to the active learning scheme. Traditional Importance Sampling (IS) is adopted to estimate the point-wise failure probability with $N = 1000$ samples for each simulation run. The results from Importance Sampling as regarded as the 'Exact' values. The proposed scheme combining an adaptive strategy and combination (denoted as AC) is compared with Weighted Importance Sampling (denoted as WIS) and Augmented Space Integral using Importance Sampling (denoted as ASI-IS). When performing comparisons, the same number of simulations is considered for each approach.

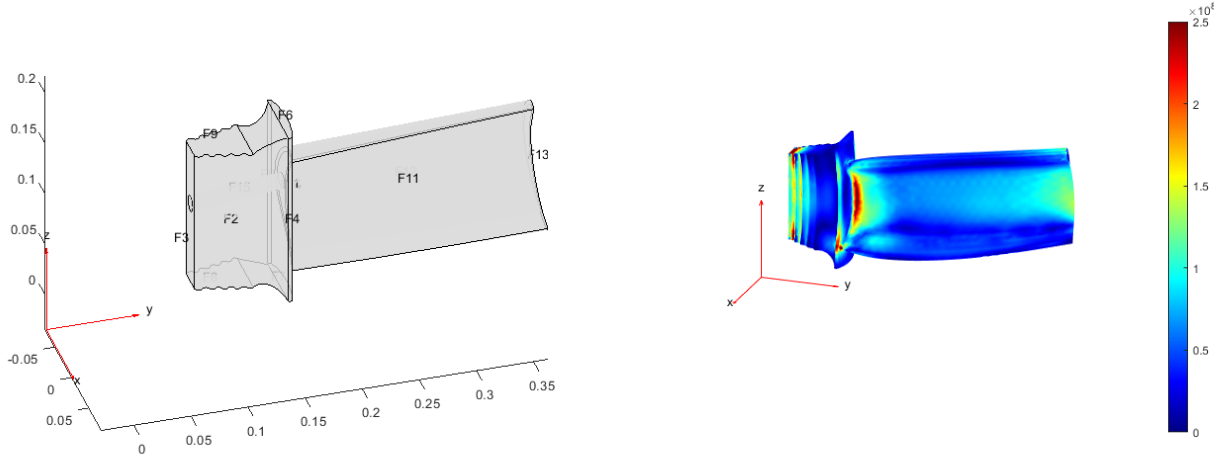

Figure 9: The geometry and von Mises stress of a turbine blade (Example 2).

Table 2: The distribution information of the basic random variables (Example 2).

Random variable	Mean value	Standard deviation
E(GPa)	$\theta_1 = \mu_E \in [170, 290]$	23
$\gamma_{CTE}(10^{-6})(1/\text{K})$	$\theta_2 = \mu_{\gamma_{CTE}} \in [10, 18]$	1.4
λ	0.27	0.027
P_1(kPa)	500	50
P_2(kPa)	450	45
K_{app}(W/m/K)	11.5	1.15
T_1(°C)	150	15
T_2(°C)	$\theta_3 = \mu_{T_2} \in [700, 1300]$	100

Fig. 10 shows the one-dimensional FPF results obtained by different methods, as well as the 'Exact' values. It is noticed that the FPF increases with all the design parameters, i.e., the mean values of Young's modulus, coefficient of thermal expansion and the temperature on the pressure and suction sides. It can be seen from Fig. 10a that the maximum of C.o.V. value by the proposed approach (AC) is less than $c_{tol} = 0.2$, while those associated with WIS and ASI-IS possess larger maximum C.o.V. values. Though the C.o.V. by the proposed AC is not necessarily the smallest among these methods for all θ_1 over the whole design region, the maximum value of C.o.V. is the smallest. In this sense, the proposed approach can obtain more smooth and consistent results under the same computational cost (in terms of the number of samples). The same phenomenon can also be seen in both Figs. 10b and 10c. The effectiveness and advantages of the proposed approach have been demonstrated through this three-dimensional FPF problem.

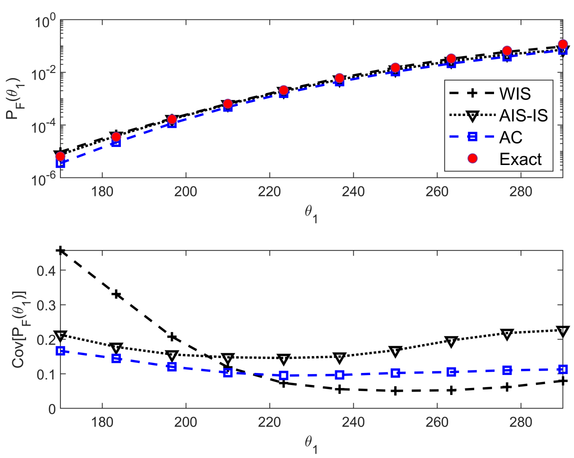

(a) $P_F(\theta_1, \theta_2 = 14, \theta_3 = 1000)$

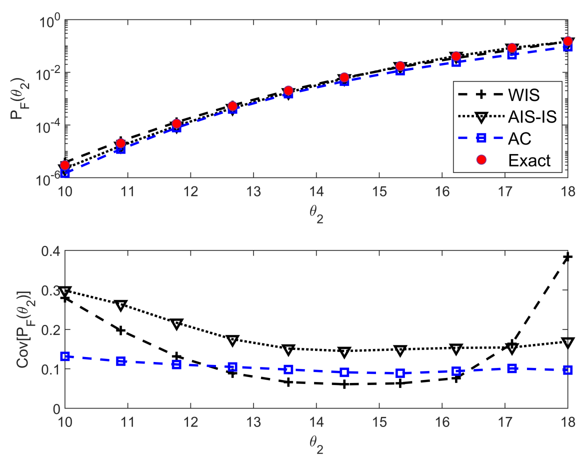

(b) $P_F(\theta_1 = 230, \theta_2, \theta_3 = 1000)$

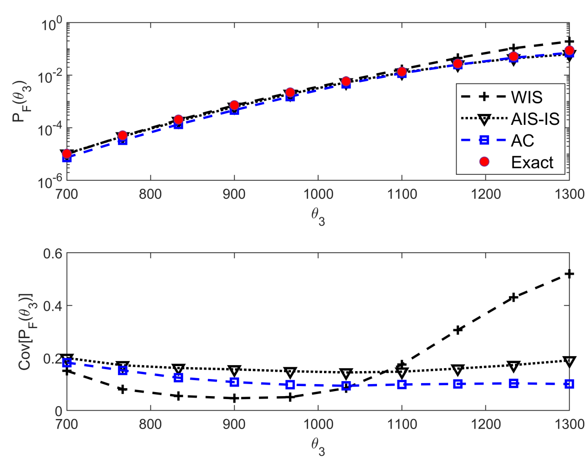

(c) $P_F(\theta_1 = 230, \theta_2 = 14, \theta_3)$

Figure 10: The one-dimensional FPF results by different methods (Example 2).

4.3. Example 3: Shear-beam oscillator

This example is taken from [27] and has been adjusted for the purposes of this work. In this example, a ten-degree-of-freedom shear-beam oscillator is considered, in which the effects of the uncertainties in both the system parameters and loading are included. The governing equation is given by:

$$\boldsymbol{M}\ddot{\boldsymbol{u}}(t) + \boldsymbol{C}\dot{\boldsymbol{u}}(t) + \boldsymbol{K}\boldsymbol{u}(t) = \boldsymbol{F}(t) \tag{21}$$

where

$$\boldsymbol{M} = \begin{bmatrix} m_1 & 0 & \cdots & 0 \\ 0 & m_2 & \cdots & 0 \\ \cdot & \cdot & \cdots & 0 \\ 0 & \cdots & 0 & m_{10} \end{bmatrix} \tag{22}$$

$$\boldsymbol{C} = \begin{bmatrix} c_1 + c_2 & -c_2 & \cdots & 0 \\ -c_2 & c_2 + c_3 & \cdots & 0 \\ \cdot & \cdot & \cdots & \cdot \\ 0 & 0 & -c_{10} & c_{10} \end{bmatrix} \tag{23}$$

$$\boldsymbol{K} = \begin{bmatrix} k_1 + k_2 & -k_2 & \cdots & 0 \\ -k_2 & k_2 + k_3 & \cdots & 0 \\ \cdot & \cdot & \cdots & \cdot \\ 0 & 0 & -k_{10} & k_{10} \end{bmatrix} \tag{24}$$

represent the mass, damping and stiffness matrices, respectively, and the random excitation has the form $\boldsymbol{F}(t) = p(t) \cdot [m_1, \cdots m_{10}]^{\mathrm{T}}$, with T indicating transpose of the argument. The random excitation possesses duration $T = 20\,\mathrm{s}$ and its discretization interval is $\Delta t = 0.05\mathrm{s}$. The values of the base random excitation at a given number of time steps constitute the vector of random parameters. Thus, there are $n_T = T/\Delta t = 401$ input random variables to discretise the excitation $\boldsymbol{F}(t)$ at time instants $t_k = (k-1)\Delta t\,(k = 1, 2, \ldots, n_T)$. It is assumed that the mass parameters $m_1, \cdots, m_{10}$ and stiffness parameters $k_1, \cdots, k_{10}$ and $\xi_1, \cdots, \xi_{10}$ are all independent (truncated) Gaussian random variables with mean values of $\mu_{m_i} = 10\mathrm{Mg}, \mu_{k_i}$ (design parameter), and $\mu_{\xi_i} = 0.04$. The standard deviations for these variables are listed in Table 3. It is also assumed that $c_i = 2\,\xi_i\sqrt{m_i k_i} \quad (i = 1, 2, \ldots, 10)$.

The uncertain excitation is modelled by a modulated filtered Gaussian white noise as follows:

$$p(t) = \omega_1^2 v_1 + 2\omega_1\zeta_1\dot{v}_1 - \omega_2^2 v_2 - 2\omega_2\zeta_2\dot{v}_2 \tag{25}$$

where

$$\frac{\mathrm{d}}{\mathrm{d}t}\begin{bmatrix} v_1 \\ \dot{v}_1 \\ v_2 \\ \dot{v}_2 \end{bmatrix} = \begin{bmatrix} 0 & 1 & 0 & 0 \\ -\omega_1^2 & -2\omega_1\zeta_1\dot{v}_1 & 0 & 0 \\ 0 & 0 & 0 & 1 \\ \omega_1^2 & 2\omega_1\zeta_1\dot{v}_1 & -\omega_2^2 & -2\omega_2\zeta_2\dot{v}_2 \end{bmatrix} \begin{bmatrix} v_1 \\ \dot{v}_1 \\ v_2 \\ \dot{v}_2 \end{bmatrix} + \begin{bmatrix} 0 \\ w(t) \\ 0 \\ 0 \end{bmatrix} \tag{26}$$

where $w(t)$ is Gaussian white noise with the autocorrelation function $E[w(t)w(t+\tau)] = I\delta(\tau)h^2(t)$ in which I denotes the intensity of the white noise, $\delta(\cdot)$ is the Dirac delta and $h(\cdot)$ is an envelope function defined as:

$$h(t) = \begin{cases} 0 & t \leq 0\,\mathrm{s} \\ t/2 & 0\,\mathrm{s} \leq t \leq 2\,\mathrm{s} \\ 1 & 2\,\mathrm{s} \leq t \leq 10\,\mathrm{s} \\ \exp[-0.1(t-10)] & t \geq 10\,\mathrm{s} \end{cases} \tag{27}$$

The values $\omega_1 = 15.0\,\mathrm{rad/s}$, $\zeta_1 = 0.8$, $\omega_2 = 0.3\,\mathrm{rad/s}$, $\zeta_2 = 0.995$, and $I = 0.08\,\mathrm{m^2/s^3}$ are used to model the filter. Failure is defined as an event where the relative displacement of the first degree of freedom exceeds $0.06\,\mathrm{m}$, and the limit state function given by

$$g(\boldsymbol{x}, \boldsymbol{z}) = b - \max_{j=1}^{n_T}(|\,Y_{1j}(\boldsymbol{x}, \boldsymbol{z})|) \tag{28}$$

where b=0.06 m; Y_{1j} denotes the structural response of the first degree of freedom at time step j; $\boldsymbol{x} = [x_1, x_2, \ldots, x_n]$ is the vector of the random variables associated with the structural parameters; $\boldsymbol{z} = [z_1, z_2, \ldots, z_{n_t}]$ is the vector of the random variables used to characterise the stochastic excitation, which are assumed as i.i.d. standard Gaussian variables in this contribution; and b_i is the i-th threshold level.

Table 3: The distribution information of the basic structural random variables (Example 3).

Random variable	Mean value	Standard deviation
k_1(MN/m)	$\theta = \mu_{k_1} \in [20, 60]$	4
$k_i(i = 2, ..., 10)$(MN/m)	40	4
$m_i(i = 1, ..., 10)$(Mg)	10	0.5
$\xi_i(i = 2, ..., 10)$	0.04	0.008

In this example, the mean stiffness μ_{k_1} is taken as the design parameter, i.e., $\theta = \mu_{k_1}$ for which the design region is $\theta = \mu_{k_1} \in [30, 60]$MN/m.

The proposed approach based on adaptive strategy and combination (AC) is applied with $N = 100$, and $c_{tol} = 0.2$. It is found that a total of $k = 9$ iterations are required to achieve convergence. Traditional Importance Sampling (IS) is also carried out to obtain the point-wise failure probabilities which are taken as the 'exact' values, where 1000 samples are used to estimate each probability value. In addition, the FPF is calculated by means of Weighted Importance Sampling (WIS) and Augmented Space Integral (ASI). Both WIS and ASI are implemented considering a total of $N_T = N \times k = 100 \times 9 = 900$ samples, in order to ensure a fair comparison with the results produced with the proposed approach. The estimates for the FPF obtained with the aforementioned methods are shown in Fig. 11. It is seen that the FPF decreases with respect to the mean value of k_1. This makes sense from a physical viewpoint, as a larger stiffness helps to control the maximum displacement. While errors exist in the results of WIS and ASI, the proposed approach obtains an accurate result that is consistent with the reference values. Meanwhile, the C.o.V. of FPF estimate by the proposed approach is smooth over the design region and it is always less than 0.2 (which is consistent with the convergence criterion set beforehand). On the contrary, the maximum values of the coefficient of variation associated with WIS and ASI are about 0.4 and 0.8, respectively. The advantage of the proposed approach is clearly shown.

5. Conclusions

This paper presents an efficient approach based on adaptive strategy and combination algorithm (AC) for structural global failure probability function (FPF) estimation. It approximates the global FPF by aggregating local estimates of FPF. These local estimates are constructed around support points which are selected in an adaptive manner. Furthermore, these local estimates are aggregated optimally according to a prescribed criterion that minimised the coefficient of variation of the global FPF estimate. The local estimation of the FPF is carried out resorting to Weighted Importance Sampling.

Through the examples addressed in this contribution, the following conclusions can be made:

- The proposed adaptive strategy is effective in identifying the design value possessing the largest C.o.V. estimator.

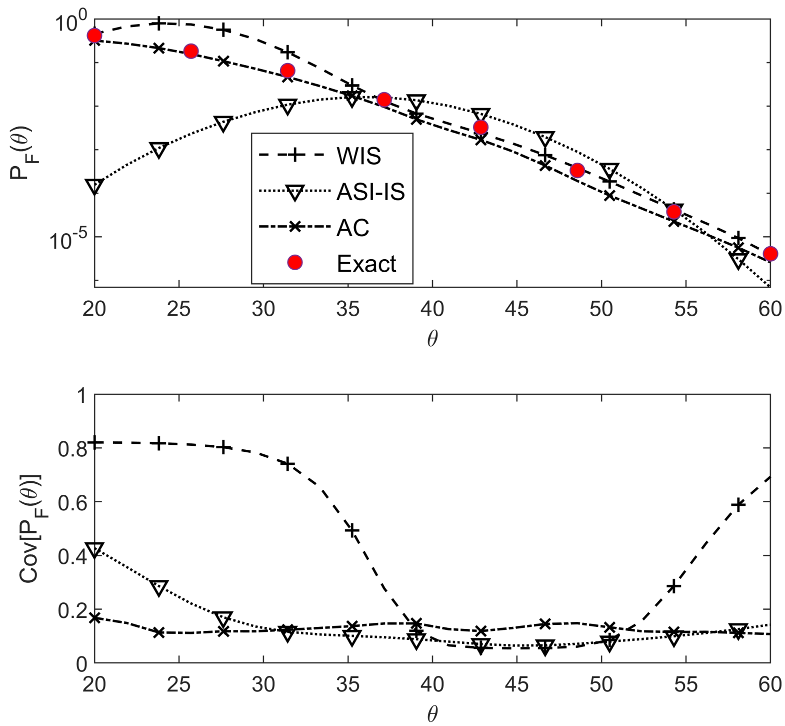

Figure 11: The FPF results by different methods (Example 3).

- The proposed optimal combination based on minimising the C.o.V. of the FPF estimate can result in an estimate with a C.o.V. smaller than any of the local FPF estimators.

- The proposed approach is numerically more efficient than the augmented space integral (ASI) method when both of them use Importance Sampling (IS) as the simulation method.

- The proposed approach is numerically more accurate than the Weighted Importance Sampling (WIS) when both of them use Importance Sampling (IS) as the simulation method.

Future research efforts will aim at expanding the scope of application of the proposed framework. For example, one possible path is exploring the assessment of local FPF estimators by means of Weighted Importance Sampling by using an adaptive Importance Sampling Density function. Furthermore, the proposed strategy can be implemented with other simulation strategies for estimating local FPF, such as weighted Monte Carlo Simulation or weighted Subset Simulation. At last, the application of the proposed approach to other problems should be explored as well, such as reliability-based design optimization and imprecise reliability estimation.

Acknowledgements

Xiukai Yuan would like to acknowledge financial support from NSAF (Grant No. U1530122), the Aeronautical Science Foundation of China (Grant No. ASFC-20170968002).

Appendix A. Selection of Weights in combination algorithm

This Appendix presents detailed deductions for the optimal weights which minimize the C.o.V. and variance as given by Eqs. (15) and (13), respectively.

As the optimization problem of minimizing the $Cov[\hat{P}_{F,C}^k(\boldsymbol{\theta})]$ is equal to minimizing the $Cov^2[\hat{P}_{F,C}^k(\boldsymbol{\theta})]$, then the optimal weights based on minimizing the C.o.V. can be stated as follows:

$$\begin{aligned} \min \quad & Cov^2[\hat{P}_{F,C}^k(\boldsymbol{\theta})] = \sum_{i=1}^{k} w_i^2(\boldsymbol{\theta}) Cov^2\left[\hat{P}_F^{(i)}(\boldsymbol{\theta})\right] \\ s.t. \quad & \sum_{i=1}^{k} w_i(\boldsymbol{\theta}) = 1 \end{aligned} \tag{A.1}$$

This problem can be solved by the method of Lagrange multipliers. The Lagrangian of the problem in Eq. (A.1) is:

$$L(\boldsymbol{w}, \lambda) = \sum_{i=1}^{k} w_i^2(\boldsymbol{\theta}) Cov^2\left[\hat{P}_F^{(i)}(\boldsymbol{\theta})\right] + \lambda\left(\sum_{i=1}^{k} w_i(\boldsymbol{\theta}) - 1\right) \tag{A.2}$$

The first-order necessary conditions for optimality read:

$$\frac{\partial L(\boldsymbol{w}, \lambda)}{\partial w_i(\boldsymbol{\theta})} = 0, \frac{\partial L(\boldsymbol{w}, \lambda)}{\partial \lambda} = 0 \tag{A.3}$$

Solving this equation will result in the following expressions

$$\begin{aligned} w_i(\boldsymbol{\theta}) &= -\frac{\lambda}{2} Cov^{-2}\left[\hat{P}_F^{(i)}(\boldsymbol{\theta})\right] \\ \lambda &= -\frac{2}{\sum_{i=1}^{k} Cov^{-2}\left[\hat{P}_F^{(i)}(\boldsymbol{\theta})\right]} \end{aligned} \tag{A.4}$$

which leads to:

$$w_i(\boldsymbol{\theta}) = \frac{Cov^{-2}\left[\hat{P}_F^{(i)}(\boldsymbol{\theta})\right]}{\sum_{j=1}^{k} Cov^{-2}\left[\hat{P}_F^{(j)}(\boldsymbol{\theta})\right]} \quad (i = 1, \cdots, k) \tag{A.5}$$

Since the objective function is convex (quadratic in w) and the constraint is affine, the result of Eq. (A.5) is the global optimum.

Similarly, the optimal weights that minimise the variance can be also obtained by solving the following optimization problem

$$\begin{aligned} \min \quad & \sum_{i=1}^{k} w_i^2(\boldsymbol{\theta}) Var[\hat{P}_F^{(i)}(\boldsymbol{\theta})] \\ s.t. \quad & \sum_{i=1}^{k} w_i(\boldsymbol{\theta}) = 1 \end{aligned} \tag{A.6}$$

and the cooresponding optimal weights are given by:

$$w_i(\boldsymbol{\theta}) = \frac{Var^{-1}\left[\hat{P}_F^{(i)}(\boldsymbol{\theta})\right]}{\sum_{j=1}^{k} Var^{-1}\left[\hat{P}_F^{(j)}(\boldsymbol{\theta})\right]} \quad (i = 1, \cdots, k) \tag{A.7}$$

Appendix B. Convergence of the optimal combination algorithm

In this Appendix, we obtain the following lemma for the estimator $\hat{P}_{F,C}^{(k)}(\boldsymbol{\theta})$ in Eq. (2) associated with the proposed optimal combination algorithm.

Lemma 1. Provided that $Cov\left[\hat{P}_F^{(j)}(\boldsymbol{\theta})\right]$ is finite, the estimator $\hat{P}_{F,C}^{(k)}(\boldsymbol{\theta})$ in Eq.(2) converges to $P_F(\boldsymbol{\theta})$ when N goes to infinity.

As $\hat{P}_F^{(i)}(\boldsymbol{\theta})$ is unbiased for each $i = 1, \cdots, k$, thus according to the central limit theory, we have

$$\lim_{N \to +\infty} \hat{P}_F^{(i)}(\boldsymbol{\theta}) = P_F(\boldsymbol{\theta}) \tag{B.1}$$

When N goes to infinity,

$$\lim_{N \to +\infty} \hat{P}_{F,C}^{(k)}(\boldsymbol{\theta}) = \lim_{N \to +\infty} \sum_{i=1}^{k} w_i(\boldsymbol{\theta}) \hat{P}_F^{(i)}(\boldsymbol{\theta}) = \sum_{i=1}^{k} \lim_{N \to +\infty} w_i(\boldsymbol{\theta}) P_F(\boldsymbol{\theta}) \tag{B.2}$$

And according to Eqs. (10) and (B.1), the limit of the weights in Eq.(B.2) becomes

$$\lim_{N \to +\infty} w_i(\boldsymbol{\theta}) = \lim_{N \to +\infty} \frac{Cov^{-2}\left[\hat{P}_F^{(i)}(\boldsymbol{\theta})\right]}{\sum_{j=1}^{k} Cov^{-2}\left[\hat{P}_F^{(j)}(\boldsymbol{\theta})\right]} = \frac{P_F^2(\boldsymbol{\theta}) \lim_{N \to +\infty} Var^{-1}\left[\hat{P}_F^{(i)}(\boldsymbol{\theta})\right]}{\sum_{j=1}^{k} P_F^2(\boldsymbol{\theta}) \lim_{N \to +\infty} Var^{-1}\left[\hat{P}_F^{(j)}(\boldsymbol{\theta})\right]} \tag{B.3}$$

$$= \frac{V_i^{-1}}{\sum_{j=1}^{k} V_j^{-1}} \tag{B.4}$$

where

$$V_i = \lim_{N \to +\infty} \left\{ \frac{1}{N} \sum_{j=1}^{N} \left[\frac{I_F\left(\boldsymbol{x}^{(j)}\right) f\left(\boldsymbol{x}^{(j)} \mid \boldsymbol{\theta}\right)}{H\left(\boldsymbol{x}^{(j)} \mid \boldsymbol{x}^{*(i)}\right)} \right]^2 - [\hat{P}_F^{(i)}(\boldsymbol{\theta})]^2 \right\} \tag{B.5}$$

$$= \left\{ \int \left[\frac{I_F(\boldsymbol{x}) f(\boldsymbol{x} \mid \boldsymbol{\theta})}{H(\boldsymbol{x}|\boldsymbol{x}^{*(i)})} \right]^2 H(\boldsymbol{x}|\boldsymbol{x}^{*(i)}) \mathrm{d}\boldsymbol{x} - [P_F(\boldsymbol{\theta})]^2 \right\} \tag{B.6}$$

It is known that $H(\boldsymbol{x}|\boldsymbol{x}^{*(i)}) \neq \frac{I_F(\boldsymbol{x})f(\boldsymbol{x}|\boldsymbol{\theta})}{P_F(\boldsymbol{\theta})}$ as it is based on design point $\boldsymbol{x}^{*(i)}$, then $V_i > 0$. Thus $\sum_{i=1}^{k} \lim_{N\to+\infty} w_i(\boldsymbol{\theta}) = 1$ also holds. Lemma 1 can be derived straightforwardly by rewriting above Eq. (B.2) as

$$\lim_{N\to+\infty} \hat{P}_{F,C}^{(k)}(\boldsymbol{\theta}) = P_F(\boldsymbol{\theta}) \sum_{i=1}^{k} \lim_{N\to+\infty} w_i(\boldsymbol{\theta}) = P_F(\boldsymbol{\theta}) \tag{B.7}$$

Note that Eq. (B.7) does not hold for an extreme case, e.g., $Cov\left[\hat{P}_F^{(j)}(\boldsymbol{\theta})\right]$ is infinite. Thus, in practical computation, these extreme cases should be taken care.

References

[1] M. Faes, D. Moens, Recent trends in the modeling and quantification of non-probabilistic uncertainty, Archives of Computational Methods in Engineering 27 (2020) 633–671.

[2] M. A. Valdebenito, H. A. Jensen, H. Hernandez, L. Mehrez, Sensitivity estimation of failure probability applying line sampling, Reliability Engineering & System Safety 171 (2018) 99–111.

[3] M. A. Valdebenito, G. I. Schuëller, A survey on approaches for reliability-based optimization, Structural and Multidisciplinary Optimization 42 (2010) 645–663.

[4] M. Gasser, G. I. Schuëller, Reliability-based optimization of structural systems, Mathematical Methods of Operations Research 46 (1997) 287–307.

[5] H. A. Jensen, Structural optimization of linear dynamical systems under stochastic excitation: a moving reliability database approach, Computer methods in applied mechanics and engineering 194 (2005) 1757–1778.

[6] M. Li, M. Sadoughi, Z. Hu, C. Hu, A hybrid gaussian process model for system reliability analysis, Reliability Engineering & System Safety 197 (2020) 106816.

[7] M. I. Radaideh, T. Kozlowski, Surrogate modeling of advanced computer simulations using deep gaussian processes, Reliability Engineering & System Safety 195 (2020) 106731.

[8] C. Cortes, V. Vapnik, Support-vector networks, Machine learning 20 (1995) 273–297.

[9] Y. Wang, X. Yu, X. Du, Improved reliability-based optimization with support vector machines and its application in aircraft wing design, Mathematical Problems in Engineering 2015 (2015).

[10] B. Echard, N. Gayton, M. Lemaire, Ak-mcs: an active learning reliability method combining kriging and monte carlo simulation, Structural Safety 33 (2011) 145–154.

[11] Q. Pan, D. Dias, An efficient reliability method combining adaptive support vector machine and monte carlo simulation, Structural Safety 67 (2017) 85–95.

[12] T. Zou, S. Mahadevan, A direct decoupling approach for efficient reliability-based design optimization, Structural and Multidisciplinary Optimization 31 (2006) 190.

[13] X. Yuan, Local estimation of failure probability function by weighted approach, Probabilistic Engineering Mechanics 34 (2013) 1–11.

[14] X. Yuan, Z. Zheng, B. Zhang, Augmented line sampling for approximation of failure probability function in reliability-based analysis, Applied Mathematical Modelling 80 (2020) 895–910.

[15] S. Au, Reliability-based design sensitivity by efficient simulation, Computers & structures 83 (2005) 1048–1061.

[16] J. Ching, Y.-H. Hsieh, Local estimation of failure probability function and its confidence interval with maximum entropy principle, Probabilistic Engineering Mechanics 22 (2007) 39–49.

[17] J. Ching, Y.-H. Hsieh, Approximate reliability-based optimization using a three-step approach based on subset simulation, Journal of engineering mechanics 133 (2007) 481–493.

[18] A. A. Taflanidis, J. L. Beck, Stochastic subset optimization for reliability optimization and sensitivity analysis in system design, Computers & Structures 87 (2009) 318–331.

[19] K. Feng, Z. Lu, C. Ling, W. Yun, An innovative estimation of failure probability function based on conditional probability of parameter interval and augmented failure probability, Mechanical Systems and Signal Processing 123 (2019) 606–625.

[20] C. Ling, Z. Lu, X. Zhang, An efficient method based on ak-mcs for estimating failure probability function, Reliability Engineering & System Safety 201 (2020) 106975.

[21] X. Yuan, S. Liu, M. A. Valdebenito, J. Gu, M. Beer, Efficient framework for failure probability function estimation in augmented space, Structural Safety 92 (2021) 102104.

[22] H. Zhang, C. Zhou, H. Zhao, Z. Zhang, An ensemble model-based method for estimating failure probability function with application in reliability-based optimization, Applied Mathematical Modelling 108 (2022) 445–468.

[23] A. Tabandeh, G. Jia, P. Gardoni, A review and assessment of importance sampling methods for reliability analysis, Structural Safety 97 (2022) 102216.

[24] R. Melchers, Importance sampling in structural systems, Structural safety 6 (1989) 3–10.

[25] I. Papaioannou, D. Straub, Combination line sampling for structural reliability analysis, Structural Safety 88 (2021) 102025.

[26] A. M. Hasofer, N. C. Lind, Exact and invariant second-moment code format, Journal of the Engineering Mechanics division 100 (1974) 111–121.

[27] G. I. Schuëller, H. J. Pradlwarter, Benchmark study on reliability estimation in higher dimensions of structural systems–an overview, Structural Safety 29 (2007) 167–182.